FROM CLASSIFICTAION RESULTS TO TOPOGRAPHIC MAPS

Joachim Höhle

Aalborg University, Department of Development and Planning, Denmark

KEY WORDS: Classification, Topographic Mapping, Cartographic Enhancement, Assessment, Accuracy

ABSTRACT:

The classification of high resolution multispectral aerial imagery enables very high thematic accuracies when machine learning methods are applied. The use of classification results as topographic maps requires cartographic enhancement and checking of the geometric accuracy. Urban areas are of special interest. The conversion of the classification result into topographic maps of high thematic and geometric quality is subject of this contribution. After reviewing the existing literature on this topic a methodology is presented. It has the goal to achieve high cartographic quality and geometric accuracy for buildings and other topographic objects. The suggested methodology for improving the classification results is described. With the ISPRS data set of the '2D labelling contest' a land cover map of six classes was produced and then enhanced by the proposed method. The classification used a machine learning method applying a variety of attributes including object heights derived from imagery. The cartographic enhancement is carried out with two different levels of quality. The user's accuracy for the classes "impervious surface" and "building" were above 85% in the 'level 1' map. The geometric accuracy of building corners in the 'level 2' map was assessed by means of reference data derived from a DSM-based orthoimage. The obtained root mean square errors were RMSE_x = 1.2 m and RMSE_y = 0.7 m. All processing could be carried out with a high level of automation.

1. INTRODUCTION

Big progress has been achieved in the classification of aerial and satellite images by means of machine learning methods. The classification results, however, are not topographic maps. Generalization of the map content and cartographic quality are absolutely necessary for topographic maps. The geometric accuracy has to meet high demands. Urban areas are of special interest. Important is also that these maps can be produced quickly and updated in short intervals of time. This demand requires automatic processing to a large extent.

In this contribution we focus on automatic 2D mapping of urban areas with detailed content including small objects. The positional accuracy of well-defined objects should be less than one meter. The graphical output must have cartographic quality, which includes simplification of the content and representation of man-made objects by straight and orthogonal lines. Such map data are in need. An overview on the status of the mapping in the world was recently published by (Konecny et al., 2015). The authors have collected data from 244 countries. In the report is stated that in the scale range "1:25000 and bigger" only 30% of the total world area is produced by the authorities. There exist big differences in the coverage with topographic maps in the mentioned scale range, e.g. 4.7% (Africa) and 98.1% (Europe). In some of the areas covered with maps or databases the data may be 10 to 30 years old. These facts demonstrate the need of improvements in the production and maintenance of such data. Private companies, e.g. Google and Microsoft, have created map data for navigation and location based services. They often use volunteers to create these maps. The Open Street Maps (OSM) is one example. The contents and accuracy of such maps differs. Tests indicate that these maps may have a geometric accuracy of 1.6m after correction of systematic errors (El-Ashmawy, 2016).

The last advancements in the sensor technology and processing methods yield new possibilities to faster produce and update the maps and databases in the important category "1:25000 and bigger". Topographic objects of urban areas need to be mapped in the scale range "1:10000 and bigger". These vector maps may be manually or automatically derived from various source data. The cartographic enhancement and the geometric accuracy are very important issues when topographic maps are the goal. This part will be the main focus point in this work. In the past, research has been carried out in order to find solutions for this task. Some authors proposed methods using lidar data only (Gross and Thoennessen, 2006; Sampath and Shan, 2007). Awrangjep et al., 2010. presented a method, which is based on aerial colour imagery **and** lidar. This contribution has the goal to automatically produce urban 2D maps of high cartographic quality and of high geometric accuracy using aerial imagery only.

The structure of the paper is the following. Section 2 describes the characteristics of topographic maps and databases. The source data and the classification methods are discussed in Section 3 and 4. The cartographic enhancement of the classification result is dealt with in Section 5. A methodology to improve the cartographic quality is presented in Section 6. Information on the assessment of the thematic and geometric accuracy is given in Section 7. Examples of cartographic enhancements are part of Section 8. Discussion and conclusion are in Section 9.

2. CHARACTERISTICS OF LARGE-SCALE TOPOGRAPHIC MAPS AND DATABASES

Topographic maps of urban areas with many details are produced in scales "1:10000 and bigger". The contents of these maps depend on the purpose of the map. Planning and management are the important applications. The various object types are stored in different layers and can be displayed individually or in combination. The storage in databases allows also an analysis of the map data. The generation and updating of such geographic information systems (GIS) is a major task of mapping organizations today. Details on the assessed accuracy, the time of acquisition, and many other information are stored in metadata. Topographic maps are always georeferenced and may also contain elevations. The separation into a planimetric

(2D) map and an accompanying digital elevation model (DEM) seems to be a trend in mapping including updating. In the following we discuss 2D maps only.

2.1 2D maps of urban areas

2D maps of urban areas are sometimes also called technical maps. Such maps should have a high geometric accuracy and a high rate of updating. They are digital vector maps and they are displayed on a computer screen in a range of scales, e.g. 1:1000 to 1:10000. Printing of analogue maps may occur on demand only. The production methods are different in the world. Manual digitizing of orthoimages is a fast and cheap method to produce and update digital vector maps today. The level of detail and accuracy of maps produced by this so-called "heads-on digitizing" depend very much on the resolution of the orthoimages. The smallest object which can be recognized should cover an area of two to three pixels which also must have sufficient contrast to its surroundings. The accuracy of orthoimages should be about two ground sampling distances (GSD). The orthoimages are often used as background information for the map data in vector format. The automatic extraction of points, lines, and areas from orthoimages is subject of this article. This process is called vectorization.

2.2 Objects of large-scale topographic maps

Objects of large-scale topographic maps are buildings, car ports, walls, roads, parking lots, paths, bridges, trees, bushes, hedges and many others. In order to represent them on a map they should have a minimum size. This is given by the resolution of the human eye which is about one minute of arc. It means that lines of 0.05 mm in width can be recognized from a distance of 30 cm. The resolution of the computer screen is given by its pixel size. For example, the pixel size of a 56 cm screen with 1680 x 1050 pixels is 0.28 mm which corresponds to a resolution of 35 pixels/cm or 90 dpi. The smallest line which can be displayed on such a screen has a width of 0.28 mm only. The lines of man-made objects must be straight and orthogonal. The lines should be without gaps and the polygons of area objects have to be closed.

3. SOURCE DATA OF CLASSIFICATION

In this contribution the generation of topographic maps is investigated by enhancing the results of classification. The resources are images, auxiliary data and usable features (attributes) of topographic objects.

3.1 Type of imagery

The images used for the classification of urban areas should have spectral bands in the visible (red, green, blue) and in the non-visible (near-infra-red) parts of the spectrum. The radiometric resolution should be better than 8 bit corresponding to 256 digital numbers. Furthermore, the images should be metric which means that accuracy values for the camera constant and the position of the principal point have to be determined by a calibration. Modern aerial photogrammetric cameras will meet these demands. The imagery has to be taken with overlap, e.g. 60%, so that heights can be derived. The ground sampling distance (GSD) should have a size that elevations can be determined with sub-meter accuracy. The taken aerial images have to be georeferenced. This means that all images will be connected by means of automatically derived homologous points. This process is called aerotriangulation which requires a few ground control points. Data of sensors for position and attitude, simultaneously recorded with the images, will support this process and enable accurate orientation data of the images. The aerial images can then be transferred into orthoimages. In this transformation, the aerial images are rectified due to their tilts and corrected for differences in terrain elevations. The first task requires the orientation data of the images and the second one needs a digital elevation model. Two elevation models can be used, either the digital surface model (DSM) or the digital terrain model (DTM). The DSM-based orthoimage depicts the buildings in a correct position but their outlines are wriggly lines. In the DTM-based orthoimage, the outlines of buildings are sharp but displaced due to the height above ground. The DTM is derived from the DSM by means of filtering. The size of the orthoimage pixel can differ from the GSD value. Each pixel of the orthoimage may have coordinates of the reference system. The coordinate value is valid either for the centre or for the upper left corner of a pixel. In order to achieve high geometric accuracies, the mentioned parameters have to be known and be correctly used in the processing.

3.2 Auxiliary data

In the following procedures in classification and graphic enhancement other data could also be used with advantage. For example, the spatial coordinates of the perspective centres and the heights above ground may be applied to correct the position of buildings when DTM-based orthoimages are used in the classification. Existing maps may be helpful to detect objects. The classification can then be restricted to certain areas, e.g. to roads and parking lots when cars have to be detected. Other data may be digital elevation models (DEMs) that are derived from airborne laser scanning (lidar) or other sensors.

3.3 Attributes and attribute profiles

The objects of topographic maps can automatically be detected by means of attributes which characterize the objects. The average height of residential houses (dZ) in suburbs may be known in advance. Other attributes used in classification are spectral signature and normalized difference vegetation index (NDVI). They can be derived from imagery. Also attribute profiles may be used. These are attributes of the standard attributes (dZ, NDVI). The attribute profiles are, for example, the standard deviation of the intensities or of elevations in the neighbourhood of a pixel.

4. CLASSIFICATION METHODS

Many classification methods have been developed in the past. Besides the generation of land cover maps with several classes, the extraction of single objects is subject of many studies. The extraction of building boundaries using high resolution images and lidar data is recently published in (Li et al., 2013). Lidar data are used to produce a coarse boundary, which is then refined by means of edges extracted from stereo images. Precise 3D boundaries of buildings are obtained by this methodology. In (Niemeyer et al., 2014) 2D building outlines are generated by means of lidar data using elevations and intensities. This investigation deals with the generation of 2D land cover maps of six classes using high resolution images only.

The applied method in this investigation is decision tree (DT). The theoretical background of the DT method is given in (Breiman et al., 1984). Experiences with DT classification are published i.a. in (Friedl and Brodley, 1997; Höhle, 2014).

5. CARTOGRAPHIC ENHANCEMENT OF THE CLASSIFICATION RESULT

In order to produce topographic maps from classification results, several steps have to be carried out. Objects which are not part of topographic maps have to be removed and topographic objects have to gain cartographic quality. The thematic and geometric accuracies of the final result have to be accessed.

5.1 Removal of non-topographic objects

Topographic maps contain permanent objects only. Cars, boats, people, animals, tents, trampolines, haystacks, and other non-permanent objects are not part of topographic maps. The classification results may have inhomogeneous areas representing more than one class. Buildings, roads, etc. have to be represented by one colour only. Non-data areas may also be present in the classification result. These areas have to be filled.

5.2 Cartographic refinements

Very small objects like garages, oriels, sheds, cellar entrances have to be removed as well. A minimum size has to be applied, e.g., area objects should cover at least 25 m^2 in nature. That means, that a simplification of the map content has to take place. The degree of this generalization will vary for different map types, which are characterized by the number of objects and their level of detail.

Man-made objects like buildings, walls, roads, etc. have to be represented in the maps or data bases by straight lines. The outlines of buildings, e.g., consist of orthogonal and parallel lines. Small deviations from linearity, orthogonality and parallelism are easily noticeable by the map user (buyer) and should therefore be corrected. All of these improvements form the cartographic quality. Research on cartographic refinement of classification results is not very much dealt with in literature. In (Li et al., 2012) a methodology is presented. By means of a DSM a building mask is derived. The corner points of buildings can then be detected and line parameters are derived from them. The orientation of the lines is then averaged for a whole district of the city.

5.3 Degree of automation

The topographic maps have to be compiled by a high degree of automation. Some manual work may still be necessary. The solutions may be different according to the demands, the available resources, and the skills of the personnel. Topographic maps and data bases of different content and levels of quality have to be considered. Computation times may also be a matter of concern. Efficient algorithms have to be found and applied.

6. A NEW METHODOLOGY TO IMPROVE CARTOGRAPHIC QUALITY

The results of the classification may be cartographically enhanced by means of image processing and image analysis techniques. Each class has to be processed for itself. Two approaches are applied in these investigations. The first approach is a simple one where the focus is on a high degree of automation, but the quality of the map is limited. We name the approach 'level 1'. The second approach, called 'level 2', yields a higher cartographic quality for buildings and other man-made objects, but the efforts become higher and some interactions by an operator are needed. The proposed solution is achieved in small steps and will be carried out at the practical tests in Section 8.

6.1 Generation of level 1

For the generation of level 1 quality only a couple of image manipulation are carried out (cf. Figure 1). Details for each step are given in the following.

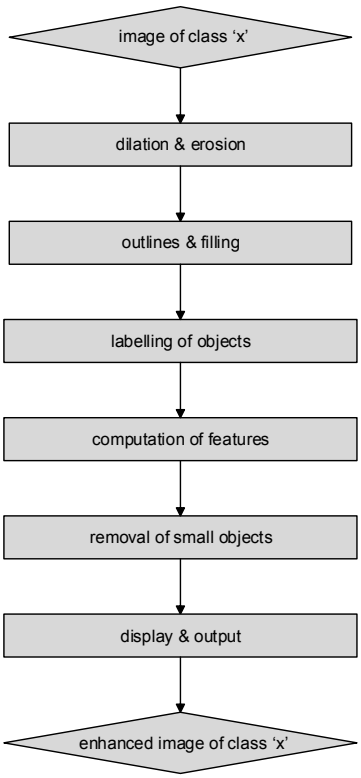

Figure 1. Steps in cartographic enhancement of land cover maps (level 1)

6.1.1 Dilation and erosion

These morphological operations are carried out by filtering. A structuring element (SE) has to be defined beforehand, e.g. a diamond shaped figure covering an area of a few pixels. The manipulations by dilation and erosion first increases the set of pixels and reduces them thereafter. The effect is a smoothing of the boundaries and a removal of some noise.

6.1.2 Outlines and filling

The first manipulation thresholds the image by means of a moving rectangular window. Two parameters have to be specified: The size of the window and the offset from the average intensity within the window. The outlines of objects are generated. The second operation generates a filling of the whole object with pixels of the intensity "1". The areas of the objects, e.g. buildings, are then homogeneous.

6.1.3 Labelling of objects

The connected sets of pixels with the intensity "1" can now be labelled by a digit. The number of objects can then be counted.

6.1.4 Computation of features

Features of objects like position, area, maximum radius, orientation, etc. are derived for each of the objects in the binary image (B). The formula for the area (A) of an object is:

$$A = \sum_{i=1}^{n} \sum_{j=1}^{m} B[i,j] \quad (1)$$

where i, j = image coordinates.

The coordinates of the centre of an object (x_c, y_c) are calculated by:

$$x_c = \frac{\sum_{i=1}^{n} \sum_{j=1}^{m} j \cdot B[i,j]}{A}$$
$$y_c = \frac{\sum_{i=1}^{n} \sum_{j=1}^{m} i \cdot B[i,j]}{A} \quad (2)$$

The units are pixels. More details about these formulas can be found in (Jain, 1995).

6.1.5 Removal of small objects

Small objects can now be removed using a threshold for the area (A) or the radius of an object. The result is a generalization of the map content.

6.1.6 Display and output

The result of three enhancements can quickly be displayed by means of the RGB-channels. Overlaps between classes can then be discovered. In order to have all classes in the map, the images have to be plotted by means of colours. The sequence of plotting should follow the rule that 'hard' objects (buildings, roads, walls) should be plotted at the end. Overlaps with the 'soft' classes (vegetation) are then repressed.

6.2 Generation of level 2

The 'level 2' approach uses results of 'level 1'and improves the lines of man-made objects. Each object has to be processed individually. It is extracted from the connected component image using its label. The point cloud of each boundary line has then to be separated from the other point clouds. The parameters of each line can now be calculated by least squares adjustment. The next step is the generation of orthogonal and parallel lines. Corner points are then calculated by intersecting successive lines. The polygons forming buildings, car ports, walls, etc. have also to be closed. The suggested approach is depicted in Figure 2 for the
class "building". It will be explained in more detail in the following.

6.2.1 Extraction of point clouds belonging to lines

The boundaries of man-made objects consist of several lines. The boundaries are approximated by straight lines. Parallel and orthogonal lines exist at buildings, walls, car ports, roads, etc.
The first step is the extraction of the point clouds forming the boundary lines. The separation of lines can be done by means of the Hough transform, which uses a voting mechanism. Each point of the point cloud votes for several combinations of parameters. The parameters that receive a majority of votes are the winners (Jain et al., 1995). The lines are modelled by

$$\rho = x \cdot \cos\theta + y \cdot \sin\theta \quad (3)$$

where ρ=distance from the origin and θ=azimuth of the normal vector to the line; *x, y* are constants in the parameter space H(θ, ρ).

All points of the point cloud of a building boundary are mapped in the parameter space using combinations of θ and ρ. The cells of the parameter space are used as an accumulator which is incremented by 1 when a point satisfies the equation (3).

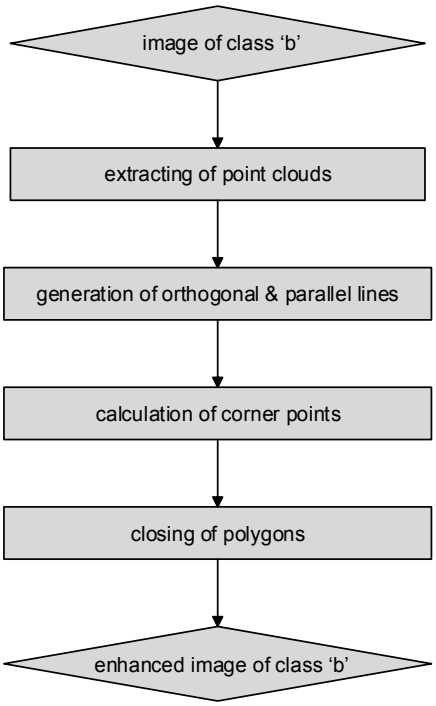

Figure 2. Steps in the cartographic enhancement (level 2) at the example of class "building"

The highest values in the accumulator array (H) correspond to the boundary lines (cf. Figure 3). The parameters are analysed in order to decide which point clouds have to be extracted so that all lines of the building can be modelled.

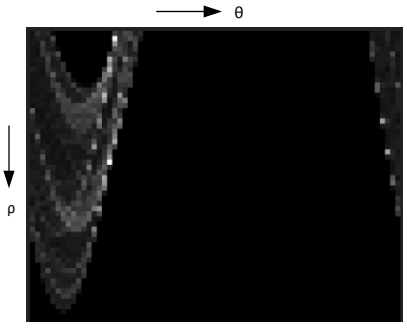

Figure 3. Display of the parameter space (H) of the Hough transform. The pixels with the highest intensities have the parameters (θ, ρ) of the building's boundary lines.

6.2.2 Generation of orthogonal and parallel lines

The extracted point clouds of building outlines are modelled by

$$a_i \cdot x + y + c_i = 0 \quad (4)$$

and coefficients (a_i and c_i) are now determined more accurately. We will use a building with four corners as an example (cf. Figure 4). Preliminary coordinates of the corner points (x_0, y_0) are obtained by intersection of two consecutive lines (l_1 and l_2).

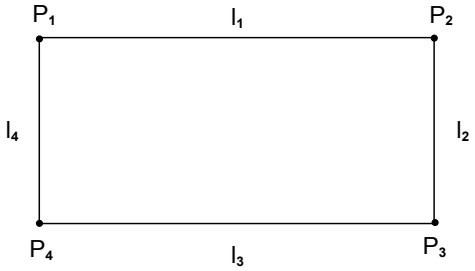

Figure 4. Sketch of building outlines and corner points

$$x_0 = \frac{c_2 - c_1}{a_1 - a_2} \tag{5}$$

$$y_0 = \frac{c_1 \cdot a_2 - c_2 \cdot a_1}{a_1 - a_2} \tag{6}$$

The final coordinates of the corner points (P_i) are derived in two steps. First, the slope value (a) is found by a weighted average

$$a = \frac{\sum_{i=1}^{n} w_i \cdot a_i}{\sum_{i=1}^{n} w_i} \tag{7}$$

where n is the number of lines and w_i is a weight. The weight is the number of extracted points for one line which about corresponds to the length of the line. The slope of the lines orthogonal to the main direction of the building are given by

$$a_{orthogonal} = -\frac{1}{a} \tag{8}$$

Such values have to be converted before the averaging. The second step calculates the c-values of equations (5) and (6) by least squares adjustment. These equations are linear and the adjustment is, therefore, very simple. The unknowns (vector $\boldsymbol{x}$) are then obtained by least squares adjustment using

$$\boldsymbol{Ax} = \boldsymbol{b} + \boldsymbol{r} \tag{9}$$

The matrix ($\boldsymbol{A}$) and the vectors ($\boldsymbol{x}$, $\boldsymbol{b}$, $\boldsymbol{r}$) have the following designations:

$$\begin{pmatrix} -k_2 & +k_2 & 0 & 0 \\ -k_1 & -k_3 & 0 & 0 \\ 0 & +k_2 & -k_2 & 0 \\ 0 & -k_3 & -k_1 & 0 \\ 0 & 0 & -k_2 & +k_2 \\ 0 & 0 & -k_1 & -k_3 \\ -k_2 & 0 & 0 & +k_2 \\ -k_1 & 0 & 0 & -k_3 \end{pmatrix} \begin{pmatrix} c_1 \\ c_2 \\ c_3 \\ c_4 \end{pmatrix} = \begin{pmatrix} x_2 \\ y_2 \\ x_3 \\ y_3 \\ x_4 \\ y_4 \\ x_1 \\ y_1 \end{pmatrix} + \begin{pmatrix} r_{x2} \\ r_{y2} \\ r_{x3} \\ r_{y3} \\ r_{x4} \\ r_{y4} \\ r_{x1} \\ r_{y1} \end{pmatrix} \tag{10}$$

The matrix elements k_1, k_2, *and* k_3 are calculated after

$$k_1 = \frac{1}{1 + a^2} \tag{11}$$

$$k_2 = \frac{a}{1 + a^2} \tag{12}$$

$$k_3 = \frac{a^2}{1 + a^2} \tag{13}$$

If there are more than four lines in the building the matrix and the vectors are extended after the same pattern. The unknown c_i-values are found by

$$\hat{\boldsymbol{x}} = (\boldsymbol{A}^T \boldsymbol{A})^{-1} \boldsymbol{A}^T \boldsymbol{b} \tag{14}$$

6.2.3 Calculation of corner points

The adjusted coordinates of the corner points are calculated by

$$\boldsymbol{p} = \boldsymbol{A}\hat{\boldsymbol{x}} \tag{15}$$

Equation 13 can be extended by a weight matrix

$$\boldsymbol{W} = diag(w_1, w_2, ...w_n) \tag{16}$$

and the unknowns (c_i) are then derived by

$$\hat{\boldsymbol{x}} = (\boldsymbol{A}^T \boldsymbol{W} \boldsymbol{A})^{-1} \boldsymbol{A}^T \boldsymbol{W} \boldsymbol{b} \tag{17}$$

The adjustment by a least squares procedure can also derive accuracy values. The estimated residuals are obtained by

$$\hat{\boldsymbol{r}} = \boldsymbol{p} - \boldsymbol{b} \tag{18}$$

from which the variance factor and the covariance matrix for the corner coordinates are derived by

$$\hat{\sigma}_0^2 = \frac{\hat{\boldsymbol{r}}^T \boldsymbol{W} \hat{\boldsymbol{r}}}{n - u} \tag{19}$$

$$\sum_p = \hat{\sigma}_0^2 \boldsymbol{A} (\boldsymbol{A}^T \boldsymbol{W} \boldsymbol{A})^{-1} \boldsymbol{A}^T \tag{20}$$

The accuracy of the corner coordinates by means of the covariance matrix is an interior accuracy only. For the assessment of the exterior accuracy we need accurate reference values.

6.2.4 Closing of polygons

The polygons have to be closed. It is achieved by repeating the first point in the list to be used in plotting.

7. ASSESSMENT OF THE THEMATIC AND GEOMETRIC ACCURACY

The assessment of the accuracies has to be carried out separately for the results of the classification, the enhanced map of level 1, and for the geometric accuracy of the enhanced map of level 2.

7.1 Assessment of the classification

The applied accuracy measures are error matrix, and overall user's and producer's accuracy. The formulas and definitions are given in (Congalton and Green, 2009).

7.2 Assessment of the enhanced maps

The assessment of the thematic accuracy by the mentioned measures can also be carried out for the enhanced map of level 1. The assessment of the level 2 results may use an accuracy measure that is based on objects. The number of objects in the scene are then compared with the detected and mapped ones.

7.3 Assessment of the geometric accuracy

The assessment of the geometric accuracy is carried out by means of the corner point coordinates. They are well-defined at a DSM-based orthoimage The accuracy measures, Root Mean Square Error (RMSE) and Mean (μ), are calculated for each of the buildings. The Mean is the average displacement of the enhanced map with regard to the reference. The comparison of the two data sets requires that an equal number of corner points exists. In reality this may not always be the case. In (Avbelj et al., 2015) a metric is proposed that evaluates the differences between polygons and line segments. This so-called 'PoLIS' method calculates orthogonal distances of vertices to line segments. We prefer the RMSE/μ as measures because of simplicity and because they are used as a standard in topographic mapping.

8. EXAMPLES OF CARTOGRAPHIC ENHANCEMENTS

The applied data are part of the ISPRS "2D semantic labelling contest" (ISPRS WG III/4, 2014). The selected test site is a city area in Germany where high buildings are close to each other. Trees, bushes and grass planes are situated between the buildings. Many cars are on roads and parking lots.

8.1 Description of source data

The original imagery is taken by a photogrammetric camera (Zeiss DMC). The images have four bands (RGB+NIR) and are of very high spatial resolution (GSD=0.09 m). The exposure occurred at sunshine which resulted in long shadows beside elevated objects. A digital surface model (DSM), a normalized digital surface model (nDSM), a false-colour orthoimage (cf. Figure 5), and a reference map were derived from the images by the organizers of the test.

Figure 5. DSM-based ortho image (false-colour)

The reference map is manually produced by means of the DSM-based orthoimage and consists of five major urban land cover classes ("impervious surfaces", "building", "low vegetation", "tree", and "car"). The selected test site covers 4 ha.

8.2 Classification

The classification starts with the training of the classifier. The chosen formula in modelling of the classes uses five variables:

$$ref \sim ndsm + ndvi + sd\_Z\_5 + b1 + sd\_b1\_5 \qquad (21)$$

where *ref*=reference class, *ndsm*=normalized digital surface model (*dZ*-value), *ndvi*=normalized difference vegetation index, *sd_Z_5*=standard deviation of the Z-value (elevation), *b1*=intensity value of the near-infrared channel (band1) of the 'true' orthoimage, *sd_b1_5*=standard deviation of the intensities of band 1 (*b1*).

The ndsm (dZ) attribute is the 'height above ground' and is calculated by

$$dZ=DSM-DTM \qquad (22)$$

The *ndvi* is derived from the intensities in the NIR-band and the Red-band according to equation (22).

$$ndvi = (I\_NIR - I\_R)/(I\_NIR + I\_R) \qquad (22)$$

where *I_NIR*=intensity in the NIR-band, *I_R*= intensity in the R-band. The units of dZ are meters (m) and of *I_NIR* and *I_R* digital numbers (DN) in the range 0-255.

The calculation of the standard deviations of the Z-values (*sd_Z_5*) and of the infra-red band (*sd_b1_5*) used the surrounding of 5 x 5 pixels of the digital elevation model and of the spectral band 1 respectively. The Z-values are not used as attributes due to the relatively big height differences of ΔZ =38 m in the area of the test site.

The decision tree (cf. Figure 6) is trained by means of an adjacent map comprising 2995 x 1783 pixels (or 4.3 ha) which contains all six classes. The class "clutter/background" consists mainly of water (river) in this area.

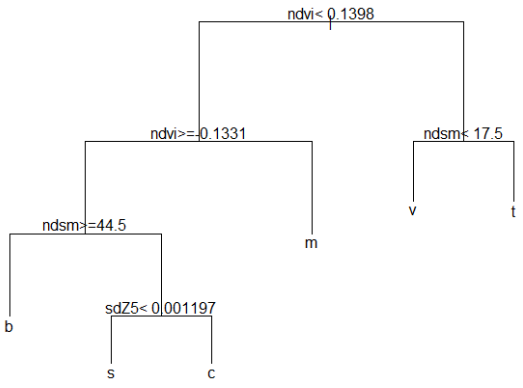

Figure 6. Decision tree derived from an existing land cover map. (b="building", s="impervious surfaces", c="car", m="clutter/background", v="low vegetation", t="tree"; sdZ5=standard deviation of elevations in the 5x5 pixels surroundings [m], ndsm=normalized digital surface model [DN], ndvi=normalized difference vegetation index.

8.3 Results

The derived accuracy measures are contained in Table 1. The user's accuracy reveals that the classes "impervious surfaces" and "building" are above 80%. The classes 'low vegetation' and "trees" are less accurate (59% and 74% respectively). The class "car" is 6% and class "clutter/background" 0% only. It means that these two classes could not be determined at all.

class	uacc [%]	pacc [%]
imp_surf	84	52
building	88	78
low_veg	59	57
tree	74	65
car	6	84
clutter	0	0

Table 1. User's accuracy (uacc) and producer's accuracy (pacc) of the test site

The overall accuracy is calculated with 64.3% (95% CI: 64.3% - 64.3%). The calculated confidence intervals (CIs) are very narrow due to the big number of checkpoints (4.93 million points). The CI-values for the user's and producer's accuracy are therefore not given.

In order to evaluate the achieved accuracy a comparison with the results of the training area are calculated (cf. Table 2).

class	uacc [%]	pacc [%]
imp_surf	79	57
building	90	73
low_veg	64	55
tree	87	87
car	8	65
clutter	67	82

Table 2. User's accuracy (uacc) and producer's accuracy (pacc) of training area.

The user's accuracy for the class "car" is also poor (8%), the class "clutter/background", however, 67%. The overall accuracy is 69.9%. It should be mentioned that the class "car" and "clutter/background" are not topographic objects and have, therefore, been removed in the cartographic enhancement.

8.4 Cartographic enhancement

The result of the cartographic enhancement (level 1) is depicted in Figure 7. It is carried out after the proposed procedures described in Section 6. For the generation of level 1 quality, the program package "EBImage" was applied (Pau, 2013). The morphological operations used a structuring element of 5 x 5 pixels. When generating the outlines of buildings, the selected parameters were 2x2 pixels (size of the moving window) and 0.01 (thresholding offset from the averaged value). The minimum area of a building to be mapped was assumed to be 25 m^2 and for the areas of class "low vegetation" 21 m^2. The areas of class "impervious surface" used as threshold a radius of 2 m and the areas of class "tree" a radius of 4 m. All objects smaller than these thresholds were removed. This generalization produces some areas of no data which have to be filled again. In this way the cartographic quality can be improved.

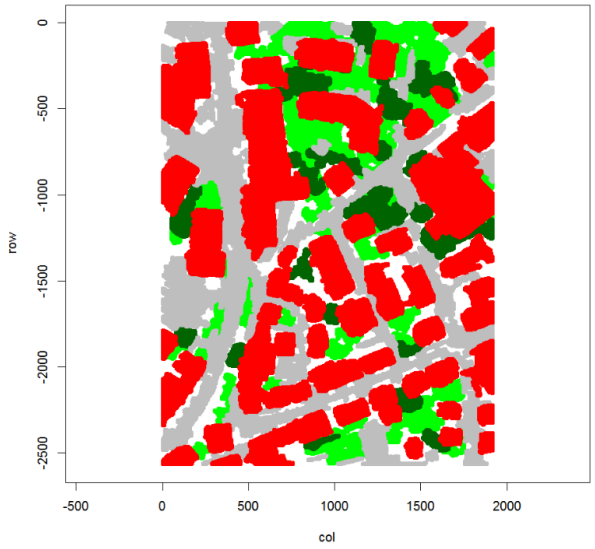

Figure 7. Enhanced land cover map - level 1. (red="building", dark green="tree", green= "low vegetation", gray="impervious surface", white= "no data")

8.5 Thematic accuracy of the enhanced map

The thematic accuracy of the topographic objects is contained in Table 3. The use of other attributes and/or thresholds may improve the results. The process of enhancement can be automated as well.

class	uacc [%]	pacc [%]
imp_surf	88	52
building	86	82
low_veg	57	58
tree	28	28

Table 3. User's accuracy (uacc) and producer's accuracy (pacc) of enhanced land cover map (level 1)

8.6 Geometric accuracy

The coordinate errors calculated from equation (19) are very small (1.0 pixel or 0.09 m). This is an interior accuracy only. The root mean square errors, derived from reference values, are absolute errors (cf. Table 4). The averages of all RMSE_x and RMSE_y are 1.2 m and 0.7 m respectively when the manually derived map (GT) was used as reference. Reference values were also derived by digitizing the corner points of buildings on top of the DSM-based orthoimage. The results are about the same. Altogether 31 corner points have been checked. The averages of the standard deviations (σ_x, σ_y) are about the same as the RMSE values. This indicates that the systematic shifts (μ_x, μ_y) of the coordinates with regard to the reference are very small. The results may be improved when a 2D transformation is applied. Besides the shifts a rotation and scale factors will then be corrected too. Building 41 includes a side the slope of which is close to 90°. In such a case, the line parameters θ and ρ are calculated. This requires a linearization of equation (3) and iterations when the approximate values of the parameters are not very accurate. Furthermore, the calculation of the corner points will then be based on equation (3) as well.

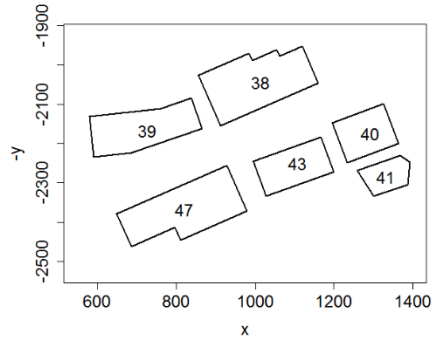

Figure 10. Enhancement of class 'building', level 2

# of building	# of corners	GT [m]		Ortho [m]	
		$RMSE_x$	$RMSE_y$	$RMSE_x$	$RMSE_y$
38	8	1.1	0.8	1.0	0.7
39	4	1.1	0.4	1.2	0.5
40	4	1.2	0.5	1.1	0.4
41	5	1.6	0.8	1.6	0.9
43	4	0.9	0.7	1.0	0.6
47	6	1.3	0.8	0.9	0.6
average	**5.2**	**1.2**	**0.7**	**1.1**	**0.6**

Table 5. Geometric accuracy of the enhanced map (level 2).

9. DISCUSSION AND CONCLUSION

The applied method used pixels of the orthoimages as units. The thematic map used for training contained six classes but was not identical with the area to be classified. The distribution of the areas of the produced land cover map was therefore different from the distribution in the training area. The obtained user's accuracy is pretty good for the classes "building" (88%) and "impervious surface" (84%). The detection of cars is poor with the selected approach. The quality of the input data and of the reference data is important for good results and should, therefore, be tested. For example, the accuracy of the elevations (Z) is of lower accuracy at the boundaries of buildings. These areas could have been ignored in the assessment. The obtainable accuracies would then definitely be higher. The cartographic enhancement improves the quality of the land cover map. The thematic accuracy is about the same for the classes "building", "impervious surfaces", and "low vegetation". The class "tree" is much worse due to the threshold for minimum area. The applied classifier (DT) could easily handle the relatively large amount of data. The processing and plotting of all classes in map-like colours required high processing times. The geometric accuracy derived from 31 corners of buildings were RMSE_x=1.2 m and RMSE_y=0.7 m. According to the positional accuracy standards for digital geospatial data, e.g. in USA, an accuracy of RMSE_x=RMSE_y=1.0m is required for map scales in the range 1: 2000 to 1:4000 (ASPRS, 2015).

REFERENCES

ASPRS, 2015. ASPRS Positional Accuracy Standards for Digital Geospatial Data, *Photogramm Eng Rem S*, 81, (3), pp. A1–A26.

Awrangjep, M., Ravanbakhsb, M., Fraser, C., 2010. Automatic detection of residential buildings using LIDAR data and multispectral imagery, ISPRS J Photogramm 65 (5), 457-467.

Avbelj, J., Müller, R., Bamler, R., 2015.A metric for polygon comparison and building extraction evaluation, *IEEE Geosci Remote S*, vol. 12, no. 1, 5 p.

Breiman, L., Friedman, J., Stone, C.J., Olshen, R.A., 1984. *Classification and regression trees*. CRC Press.

Congalton, R., G, Green, K., 2008. *Assessing the accuracy of remotely sensed data*. CRC Press.

El-Ashmawy, K. L. A., 2016. Testing the positional accuracy of OpenStreetMap data for mapping applications, *Geodesy and Cartography*, vol. 42, issue 1, pp. 25-30.

Friedl, M.A., Brodley, C.E., 1997. Decision tree classification of land cover from remotely sensed data. Remote Sens. Environ. 61, 399–409.

Gross, H., Thoennessen, U., 2006. Extraction of lines from laser point clouds, In: Symposium of ISPRS Commission III: Photogrammetric Computer Vision PCV06. *International Archives of Photogrammetry, Remote Sensing and Spatial Information Sciences,* pp. 86-91.

Höhle, J., 2014. Generation of 2D land cover maps for urban areas using decision tree classification, *ISPRS Annals of the Photogrammetry, Remote Sensing and Spatial Information Sciences*, vol. II-7, pp. 15-21.

ISPRS WG III/4, 2014. http://www2.isprs.org/commissions/comm3/wg4/semantic-labeling.html (12 June 2016).

Jain, R., Kasturi, R., Schunck, B.G., 1995. *Machine vision*, McGraw-Hill, Inc., ISBN 0-07-113407-7.

Konecny, G.; Breitkopf, U.; Radtke, A.; Lee, K., 2015. The status of topographic mapping in the world - a UNGGIM-ISPRS project 2012-2015, final report, Leibniz Universität Hannover, 64 pp.

Li, H., Zhong, C., Hu, X., Xiao, L., Huang, X., 2013. New methodologies for precise building boundary extraction from LiDAR data and high resolution image. *Sensor Rev*, 33/2, pp. 157-165.

Li, Y., Zhu, L., Shimamura, K., Tachibana, K., 2012. A refining method for building object aggregation and footprint modelling using multi-source data. *International Archives of the photogrammetry, remote sensing and spatial information sciences*, vol. XXXIX-B3, pp.41-46.

Niemeyer, J., Rottensteiner, F., Soergel, U., 2014. Contextual classification of lidar data and building object detection in urban areas. *ISPRS J Photogramm* 87, pp. 152-165.

Pau, G., Sklyar, O, and W. Huber, 2013. Introduction to EBImage - an image processing and analysis toolkit for R, http://www.bioconductor.org/packages/release/bioc/html/EBImage.html (13 June 2016)

Sampath, A., Shan, J., 2007. Building boundary tracing and regularization from airborne LiDAR point clouds. Photogramm Eng Remote S 73 (7), pp. 805-812.

ACKNOWLEDGEMENT

The author thanks the ISPRS WG III/4 for providing test data.